COBEM 2021 26th International Congress of Mechanical Engineering
November 22-26, 2021, Virtual Congress, Brazil

COB-2021-1053
Differential evolution optimization of periodic micro-perforated chamber mufflers for low-frequency sound attenuation

Adriano Mitsuo Goto
José Maria Campos Dos Santos

University of Campinas (UNICAMP)
a228247@dac.unicamp.br

Abstract. *Low-frequency noise is common as background noise in industrial and urban environments. Due to its properties of low acoustic dissipation and high propagation effectiveness, the control of this particular noise is a recurrent challenge in acoustic design. An interesting solution is the use of micro-perforated elements. The submillimetric dimensions of the holes provide a high acoustic resistance and a low acoustic reactance which enhance the sound attenuation at lower frequencies. For duct noise problems, the concept of micro-perforated elements can be used in conventional reactive-type silencers, such as chamber mufflers by inserting an internal micro-perforated duct. This setup, called micro-perforated chamber muffler (MPCM) also exhibits interesting phononic crystals (PCs) behavior when set periodically. The periodic arrangement provides the appearance of bandgap regions where the waves cannot propagate. Therefore, the acoustic performance of MPCM can be improved by combining the periodicity and the dissipation effects. For the present paper, the forced response, the transmission loss, and the dispersion diagram are evaluated for periodic MPCM systems by using an alternative transfer matrix approach. Numerical cases are computed and validated with the Finite Element method. The influence of geometric parameters is investigated and the differential evolution optimization is implemented in order to increase the acoustic performance for the low-frequency range. Simulated results show a considerable improvement of the sound attenuation at frequencies below 500Hz at feasible geometric dimensions.*

Keywords: *Micro-perforated duct, Chamber muffler, Periodic systems, Differential evolution, Transfer matrix method.*

1. INTRODUCTION

The use of perforated elements has been used for decades as acoustical elements to provide additional sound attenuation. However, perforations in the order of magnitude of centimeters do not provide high dissipation of acoustic energy. Maa (1975, 1987, 1998) was the first researcher to propose exact and approximate impedance expressions for micro-perforated elements, with perforations in the order of magnitude smaller than millimeters, showing that submillimeter holes can provide high acoustic resistance and low mass reactance. Since then, several works about micro-perforated elements (MPE) have been published due to their potential applications. The MPE is considered a future substitute for porous materials as they exhibit similar absorption characteristics while do not show operational limitations such as small particle discharge and bacterial contamination.

Despite Maa's investigation focused on acoustic panels, widely used in environmental noise control, the MPE can be extended to several acoustic filters and for various applications. For duct noise problems, Wu (1997) proposed equations to predict sound attenuation of the micro-perforated duct and analyze the effect of geometric parameters on the silencer performance. Allam and Abom (2011) investigated models for the acoustic impedance of micro-perforated ducts with circular and split-shaped holes. Bravo *et al.* (2016) proposed an extension of the Multi-Modal Propagation method to simulate and optimize a micro-perforated cylindrical silencer in the linear and nonlinear regime. Shi and Mak (2017) investigated the acoustical attenuation of a periodic array of micro-perforated tube muffler and analyzed some geometric parameters on the transmission loss with experimental validation. In recent work, Lu *et al.* (2017) proposed a new design for a compact micro-perforated muffler with a serial-parallel coupling mode for automobile engines. (Kim and Ih, 2020) proposed a compact duct silencer for square-shaped ducts coupling micro-perforated panels on the lateral surface. And Chen *et al.* (2020) have optimized micro-perforated silencers for engine intake noise control using a genetic algorithm-based called Differential Evolution (DE).

The DE method is a gradient-free optimization technique for solving complex optimization problems. This method is a population-based algorithm that searches the optimum point by randomly mutating the population and selecting the best individual at each generation (Storn and Price, 1997; Bilal *et al.*, 2020). The DE is a versatile and flexible method that provides an optimal solution for most real problems where the gradient derivation is impracticable.

The objective of the present work is to extend the previous analysis of chamber mufflers with internal micro-perforated

ducts (Goto and Santos, 2019), called micro-perforated chamber mufflers (MPCM), by optimizing this silencer using the DE algorithm. The objective function is obtained from the transmission loss response derived by a transfer matrix-based method. The single, periodic and aperiodic MPCM systems are optimized for the low-frequency range. Results show a significant improvement in the acoustic efficiency at feasible geometric dimensions.

2. MATHEMATICAL MODEL

Figure 1 shows a scheme of a micro-perforated chamber muffler, which is a combination of a expansion chamber with an inner micro-perforated duct. Note that acoustic pressure and mass velocity are different in duct and chamber. Assuming

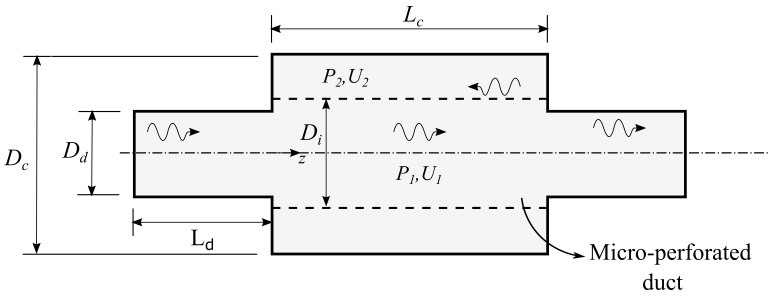

Figure 1. Micro-perforated chamber muffler scheme.

plane wave propagation inside both micro-perforated duct and chamber, the coupled system governing equation can be expressed as (Wu, 1997; Sullivan and Crocker, 1978):

$$\begin{aligned} &\frac{d^2P_1}{dx^2} + \left(k^2 - j\cdot\frac{4}{D_i}\frac{k}{\zeta}\right)P_1 + j\cdot\frac{4}{D_i}\frac{k}{\zeta}P_2 = 0, \\ &\frac{d^2P_2}{dx^2} + j\cdot\frac{4D_i}{D_c^2 - D_i^2}\frac{k}{\zeta}P_1 + \left(k^2 - j\cdot\frac{4D_i}{D_c^2 - D_i^2}\frac{k}{\zeta}\right)P_2 = 0, \end{aligned} \tag{1}$$

where D_i, D_c and D_d are the diameters of the internal duct, the chamber and of the inlet/outlet ducts. Also, P_1 and P_2 are the acoustic pressure before and after the micro-perforation, respectively. And ζ is the specific acoustical impedance of the micro-perforation expressed as (Maa, 1998):

$$\zeta = \frac{32\eta}{\sigma\,\rho_o\,c_o}\frac{t}{d_h^2}\left[\sqrt{1+\frac{K^2}{32}} + \frac{\sqrt{2}}{32}K\frac{d_h}{t}\right] + j\cdot\frac{\omega\,t}{\sigma\,c_o}\left[1 + \frac{1}{\sqrt{9+\dfrac{K^2}{2}}} + 0.85\frac{d_h}{t}\right], \tag{2}$$

where $K = d_h\sqrt{\omega\rho_o/4\eta}$, $\sigma = N_h A_h/A_L$, η is the viscosity of air, σ, d_h and t are porosity, hole diameter and micro-perforated duct thickness, respectively. Also, N_h is the number of holes, A_h and A_L are hole and duct surface areas, respectively.

The (1) can be rewritten as a space-state form as follows:

$$\frac{d}{dx}\begin{Bmatrix} P_1 \\ -v_1 \\ P_2 \\ -v_2 \end{Bmatrix} = \begin{bmatrix} 0 & j\cdot kY_1 & 0 & 0 \\ \dfrac{4}{D_d\,\zeta\,Y_1} + j\cdot\dfrac{k}{Y_1} & 0 & -\dfrac{4}{D_d\,\zeta\,Y_1} & 0 \\ 0 & 0 & 0 & j\cdot kY_2 \\ -\dfrac{4D_d}{(D_c^2 - D_d^2)\,\zeta\,Y_2} & 0 & \dfrac{4D_d}{(D_c^2 - D_d^2)\,\zeta\,Y_2} + j\cdot\frac{k}{Y_2} & 0 \end{bmatrix}\begin{Bmatrix} P_1 \\ -v_1 \\ P_2 \\ -v_2 \end{Bmatrix}, \tag{3}$$

where $v_j = \rho_0 S_j U_j$ is mass velocity and $Y_j = c_0/S_j$ is the characteristic impedance with S_j representing the cross-sectional area of the internal duct or the chamber ($j = 1, 2$).

The transfer matrix can be obtained numerically. However, the Eq. (1) gives a 4×4 matrix. To reduce to an 2×2 matrix, the following boundary conditions are applied:

$$\begin{cases} v_2(0) = 0, \\ v_2(L_c) = 0. \end{cases} \tag{4}$$

Then, the transfer matrix for micro-perforated chamber muffler is given as:

$$\mathbf{T}_m = \begin{bmatrix} T_{11} - \frac{T_{13}T_{41}}{T_{43}} & T_{12} - \frac{T_{13}T_{42}}{T_{43}} \\ T_{21} - \frac{T_{23}T_{41}}{T_{43}} & T_{22} - \frac{T_{23}T_{42}}{T_{43}} \end{bmatrix}, \tag{5}$$

where T_{ij} with $i, j = 1, \ldots, 4$ are the terms of the 4×4 transfer matrix.

The transmission loss coefficient can be computed directly from the total transfer matrix of the structure. The total TM ($\mathbf{T}_t$) is computed by multiplying the cell transfer matrices of each cell arranged along the structure. Once $\mathbf{T}_t$ is obtained, the transmission loss is given as:

$$\mathrm{TL} = 20 \log_{10} \left(\frac{1}{2} \left| T_{11} + \frac{T_{12}}{Y} + Y T_{21} + T_{22} \right| \right), \tag{6}$$

with $Y = c_0 / S_d$ where S_d is the transversal area of the inlet/outlet duct.

Moreover, for the forced response, the pressure at the ends are computed as

$$\begin{Bmatrix} P_1 & P_N \end{Bmatrix}^T \mathbf{D} = \begin{Bmatrix} v_1 & v_N \end{Bmatrix}^T, \tag{7}$$

where $\mathbf{D}$ is the condensed dynamic stiffness matrix of the structure calculated from the transfer matrix $\mathbf{T}_t$ (Silva *et al.*, 2016).

3. DIFFERENTIAL EVOLUTION OPTIMIZATION

For the optimization, several constructive parameters of the MPCM cell was subject for variation on the Differential Evolution (DE) method. Fig. 2 shows the optimization parameters and the profile of MPCM silencer and Tab. 1 shows the minimum and maximum values of each constructive parameter used in the optimizations. The inlet/outlet duct diameter was not subject to optimization since they are considered part of the mainstream duct. Therefore, the duct diameter D_d was fixed at 40 mm.

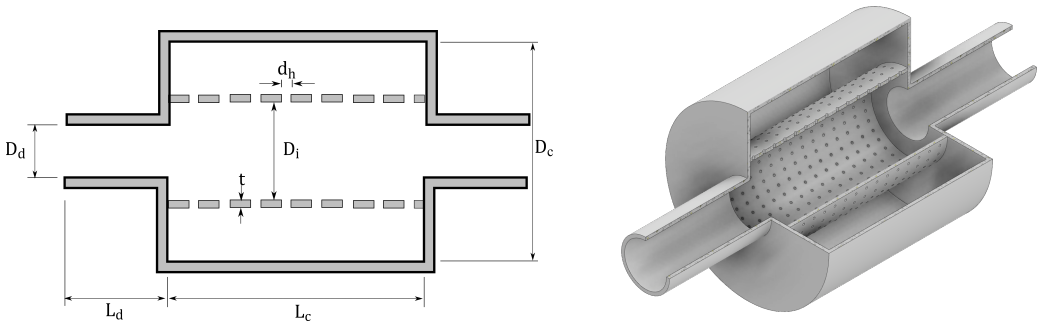

(a) Constructive parameters of MPCM (b) Profile of a MPCM cell

Figure 2. Schematic view of MPCM silencer.

Table 1. Value of the constructive parameters subject to optimization.

Value of the constructive parameters	D_c [mm]	D_i [mm]	L_c [mm]	L_d [mm]	d_h [mm]	t [mm]	N_f
Minimum	100	40	50	50	0.25	1	50
Maximum	200	150	500	500	1.00	3	1000

For the optimization process, the objective function is the integral of the transmission loss curve in the determined frequency range. Since the transmission loss (TL) function has no explicit dependence on the frequency, the integral was computed numerically using the trapezoidal integration method. The value of the are below the TL curve is divided by the frequency range. Therefore, the objective function is given as:

$$\text{Max } F(x_1, \ldots, x_n, f) = \frac{\int_{f_0}^{f_{max}} TL(f) df}{f_{max} - f_0}, \qquad i = 1, \ldots, n \tag{8}$$

where f_0 and f_{max} are the initial and the final frequency value of the analyzed range. While x_i are the constructive parameters of the MPCM.

The objective function can be interpreted as the average TL on the determined frequency range. However, it was observed that the integration provides a more stable solution than just computing directly the mean TL. In other words, the solution converges to an optimal point even though each optimization has a different initial population.

4. NUMERICAL RESULTS

The present section exhibits the numerical results obtained from the optimization of MPCM using the DE algorithm. For the simulation, it was considered the standard air properties (density $rho = 1.204$ kg/m^3, sound speed $c_0 = 343.3$ m/s and dynamic viscosity $\eta = 1.84 \times 10^{-5}$ Pa s). The damping effect represented by the air dynamic viscosity was included in the wavenumber of the plane wave as $\bar{k_0} = k_0(1 - j \cdot \eta/2)$. For comparison purposes, it was used the constructive parameters of the previous work (Goto and Santos, 2019). In the present study, these geometric values are considered "standard". For the optmization process, the number of generations was fixed at 150 and the objective function was evaluated at the frequency range of 1-500Hz. Furthermore, the mutation constant (f) and factor (CR) were set 0.5 and 0.75, respectively.

4.1 Validation of the numerical method

The validation of the transfer matrix approach was carried by comparing the results obtained with the finite element (FE) method evaluated in the COMSOL Multiphysics 5.6. The transmission loss for infinity and finite structures were computed. For the finite structure, it was evaluated the case of a single cell and of a periodic structure with 5 cells. Both cases with standard dimensions. Figure 3 presents the validation of the transmission loss curves. It can be observed that both finite structure cases ($N_c = 1, 5$) exhibit excellent agreement with the FE results. Moreover, it can be noted that a structure with 5 cells shows a good approximation for the infinity structure case.

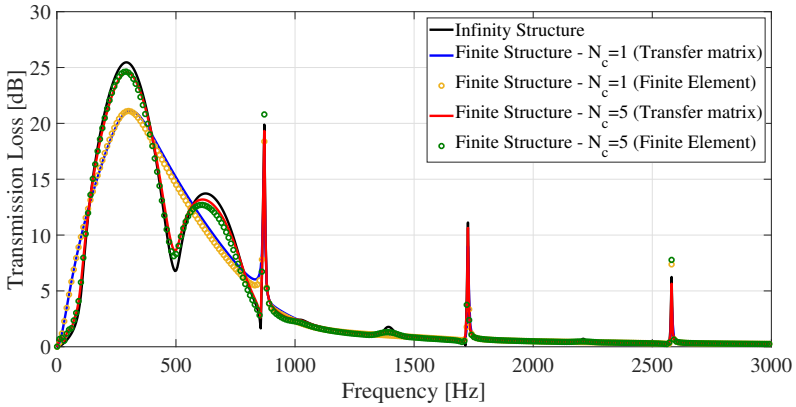

Figure 3. Validation of the transmission computed for infinite and finite structures ($N_c = 1, 5$) by the transfer matrix and the finite element methods.

4.2 Case 01: Optimization of a single cell

In the first analysis, it was considered the case of a single MPCM silencer added in the main duct where the fluid is flowing. For this reason, the length of the inlet and outlet duct was not subject to optimization. The optimized parameters are shown in Tab.2. The chamber diameter has a similar effect as in a conventional expansion chamber muffler, where a greater expansion ratio provides a higher attenuation level. This behavior also affects the internal diameter where, at the end of 150 generations, the best design showed an internal duct diameter equal to the inlet/outlet duct diameter. Moreover, it was also observed that the optimum perforation diameter reaches the maximum allowed value, i. e, 1 mm. It is because that a smaller diameter shifts the main attenuation region to lower frequencies but decreases its level. Once the DE algorithm searches for a high attenuation average, silencers with greater perforation diameter are more likely to pass their genes to the next generation. Besides that, it can be observed that is not necessary to use a thick micro-perforated duct to provide a high attenuation band neither a considerable number of perforations.

Table 2. Constructive parameters of the standard and optimized MPCMs for the single-cell case.

Value of the constructive parameters	D_c [mm]	D_i [mm]	L_c [mm]	L_d [mm]	d_h [mm]	t [mm]	N_f
Standard	150	40	200	100	0.75	2	300
Case 01 - Single cell	199.79	40.01	205	100	1	1.46	290

The results of the optimization of a single cell are shown in Fig.4. As noted, for the TL curve at Fig.4a, although the bandwidth of attenuation remains equal, the acoustic performance has improved considerably at the frequency range 1-850Hz. Moreover, the attenuation level has increased by 20% at the frequency of 310Hz, where is the peak of absorption for the standard design. And the maximum attenuation level has been increased by 50% for the optimized design. These

improvements on the TL curve are also observed on the forced response (or frequency response function - FRF). For the FRFs curves, it was considered known inlet and outlet mass velocities and anechoic conditions at the end of the structure, where the pressure P_N is evaluated and divided by the inlet mass velocity v_1. As can be noted, the first attenuation band is increased up to 850Hz and the FRF level decreased 10dB more than the standard case.

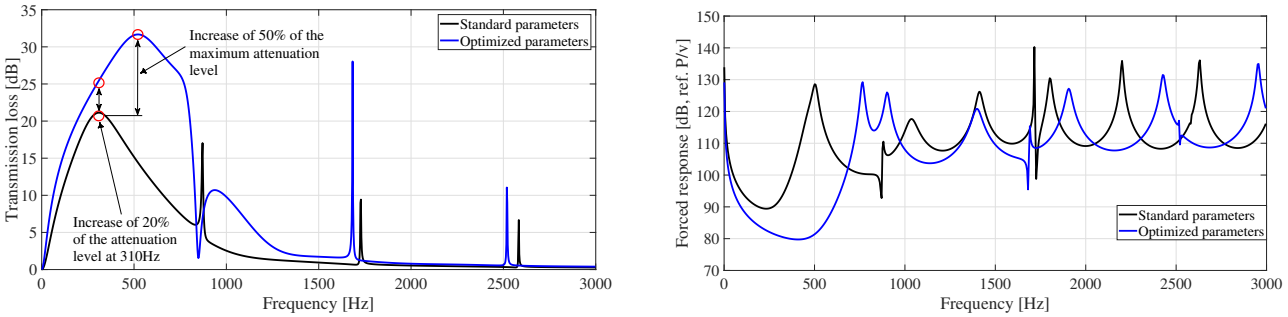

(a) Transmission loss (b) Forced response

Figure 4. Transmission loss and forced response curves for standard and optimized MPCM for the optimization of a single cell case.

4.3 Case 02: Infinity case

The values of the optimized parameters are exhibited in Tab.3. As observed for the single-cell case, chamber and internal duct diameters reached the maximum and minimum values. Also, the number of perforations and the thickness of the micro-perforated duct showed similar values compared to the previous case. On the other hand, the chamber and inlet/duct lengths were decreased showing that it is not necessary for a long silencer structure to provide good sound attenuation.

Table 3. Constructive parameters of the standard and optimized MPCMs for the infinity structure case.

Value of the constructive parameters	D_c [mm]	D_i [mm]	L_c [mm]	L_d [mm]	d_h [mm]	t [mm]	N_f
Standard	150	40	200	100	0.75	2	300
Case 02 - Periodic structure	199.99	40.00	167.87	50	1	1	271

Figure 5a, it can be observed that both attenuation level and its bandwidth increase. The attenuation level has increased about 47% while the bandwidth has improved around 27%. It is important to note that even though it was computed for an infinity number of periodic cells, it is necessary for only 5 cells to converge to the TL curves, as already presented in Fig.3. In addition, the FRF curve, as shown in Fig.5b, exhibit an excellent decrease of the response in the first attenuation band.

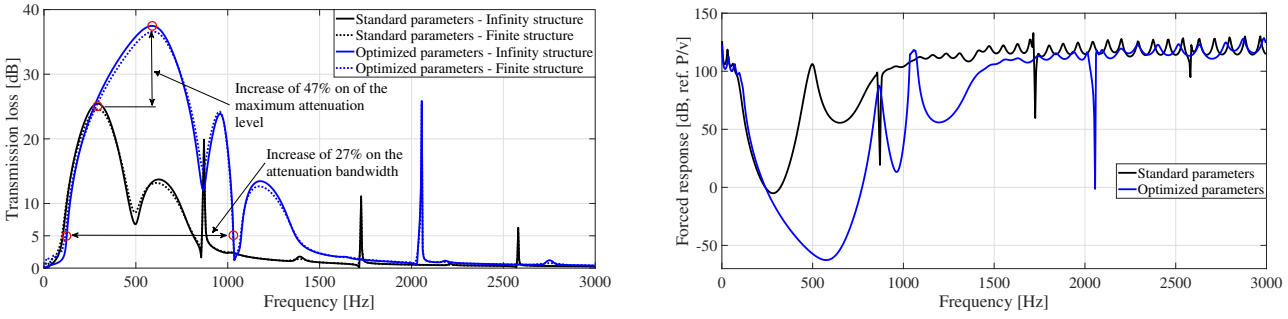

(a) Transmission loss (b) Forced response

Figure 5. Transmission loss curve for standard and optimized MPCM for the optimization of a infinity periodic structure.

Figure 6 shows the dispersion diagram for the standard and for the optimized structures. The dispersion diagram describes the behavior of the wave propagating in the structure by evaluating the real and the imaginary part of the Brag wavenumber in the frequency spectrum. The Brag wavenumber (k_B) represents the wavenumber of the unit-cell and can be computed by solving an eigenvalue problem assuming the Floquet-Bloch periodic conditions. For pure reactive silencers, as conventional expansion chamber mufflers, the attenuation region can be predicted at the regions where the real part of k_B assumes a constant value (π or 0) and the imaginary part has a non-null value, showing a pure evanescent

behavior of the wave in that frequency band, commonly called stop-band or bandgap. For MPCM silencers, the bandgaps exhibit an unusual profile due to the dissipation effects where the sound still keeps being attenuated even presenting a propagating term, as can be observed in Fig.6. Moreover, the optimized structure exhibits a significant enhancement on the bandgap width and on the level ($\Im[k_B h] < -3$).

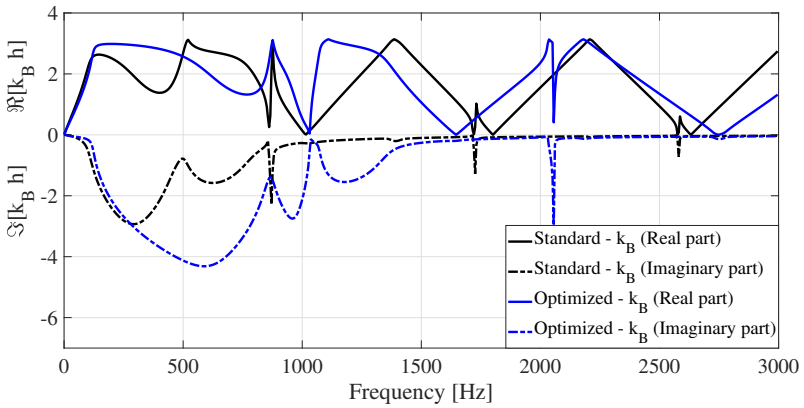

Figure 6. Dispersion diagram for standard and optimized MPCM.

4.4 Case 03: Finite structure of independent cells

The results of the optimization of a structure with 5 independent cells, Tab.4, showed that the structure does not converge over generation to a periodic arrangement even increasing the number of generations. Despite the values of some parameters, like duct length and thickness, which seem to be reached randomly, the values of the chamber length and the number of perforations exhibit some sort of increasing-decreasing behavior over the cells. For the chamber length, particularly, it was observed that the values tend to be symmetric in relation to the middle cell (cell 03). That behavior was observed over several optimization trials showing that the solution has converged to an optimal design.

Table 4. Constructive parameters of the standard and optimized MPCMs for finite structure of independent cells.

Value of the constructive parameters	Cell	D_c [mm]	D_i [mm]	L_c [mm]	L_d [mm]	d_h [mm]	t [mm]	N_f
Standard		150	40	200	100	0.75	2	300
	1	200	40.00	303.1	370.4	1	2.9	351
	2	200	40.00	299	498.7	1	2.9	335
Case 03: Independent cell	3	199	40.00	497.4	50	1	2.8	448
	4	198	40.00	298.8	413.8	1	1	160
	5	200	40.00	303.6	50	1	1	159

Figure 7 shows the TL and FRF results for the standard and optimized structures. As observed in Fig.7a, the main improvement is at the increase of the bandwidth of attenuation especially shifting it for frequencies below 100Hz. The attenuation level also exhibited an improvement around 23% at 440Hz, but not as substantial as shown for the periodic case. However, these nearly-random parameter values provided a substantial attenuation of the FRF curve at the range 1-500Hz, as exhibited in Fig.7b.

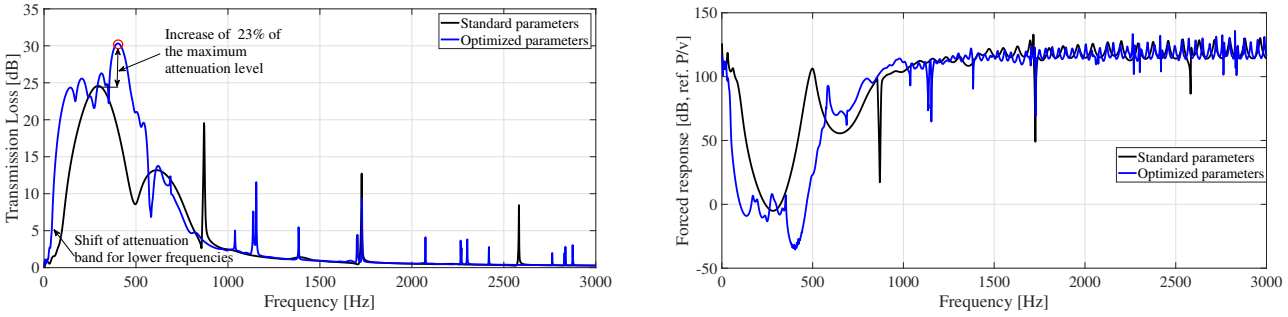

(a) Transmission loss (b) Forced response

Figure 7. Transmission loss curve for standard and optimized MPCM for the optimization of a finite structure of independent cells.

4.5 Case 04: Graded-like finite structure

For the last optimization case, it was evaluated a finite structure where the dimensions of the MPCM cells varying slowly over the arrangement. This building concept of the nearly periodic structure is has been commonly called a rainbow or graded metamaterial. Several papers has been published investigating the elastic and acoustic performance of graded-like metamaterial (Meng *et al.*, 2020; Fabro *et al.*, 2021; Hu *et al.*, 2021). Since nearly-periodic structure tends to show a better wave attenuation than periodic structures (Langley, 1995), the last optimization was performed considering a scale factor η for some constructive parameters that describe how bigger or smaller the dimension of the last cell is in comparison to the first one. Table 5 shows the maximum and minimum values for each scaling factor. It was considered scaling up to 50% on the last cell except for the chamber length and perforation diameter since the optimization tends to select the maximum allowed values. Also, for the internal duct diameter, it was considered only an increase in its value due to constructive limitations, i.e, it is not possible that the internal duct has a smaller diameter than the inlet/outlet duct.

Table 5. Value of the scaling factors subject to optimization for graded-like structure.

Scaling factors for constructive parameters	η_{D_c}	η_{D_i}	η_{L_c}	η_{L_d}	η_{d_h}	η_t	η_{N_f}
Minimum	0.5	1	0.5	0.5	0.5	0.5	0.5
Maximum	1	1.5	1.5	1.5	1	1.5	1.5

The results of the last case are shown in Tab.6. The values of the constructive parameters are similar to the optimization of the infinity structure. The main difference is in the scale factors. The scale factors for chamber diameter, inner duct, and bore remain equal to 1 showing that the optimization has reached the maximum/minimum value allowed. In addition, chamber length exhibited a 10% increase across the cells, while duct length decreased by 50%, showing the silencers getting closer together after the first cell. Meanwhile, the internal duct thickness and the number of perforations provided a balance of the total acoustic impedance.

Table 6. Constructive parameters of the standard and optimized MPCMs for graded-like structure case.

Value of the constructive parameters	D_c [mm]	D_i [mm]	L_c [mm]	L_d [mm]	d_h [mm]	t [mm]	N_f
Standard	150	40	200	100	0.75	2	300
Case 04 - Graded-like structure	200	40	191.1	50	1	1	368
Value of the scaling factors	η_{D_c}	η_{D_i}	η_{L_c}	η_{L_d}	η_{d_h}	η_t	η_{N_f}
	1	1	1.1	0.5	1	1.5	0.61

Figure 8 presents the TL and FRF results for the graded-like structure. Despite the fact the values of the optimized parameters are similar to the optimized values for the infinity structure case, the TL curve in Fig.8a exhibits a considerable improvement on the attenuation level and on its bandwidth. The maximum transmission loss reached around 40dB at 510Hz which is a good performance. Besides, the attenuation band has increased around 57% considering the attenuation level of 5dB level. While the FRF exhibits an increased attenuation region below 1000Hz.

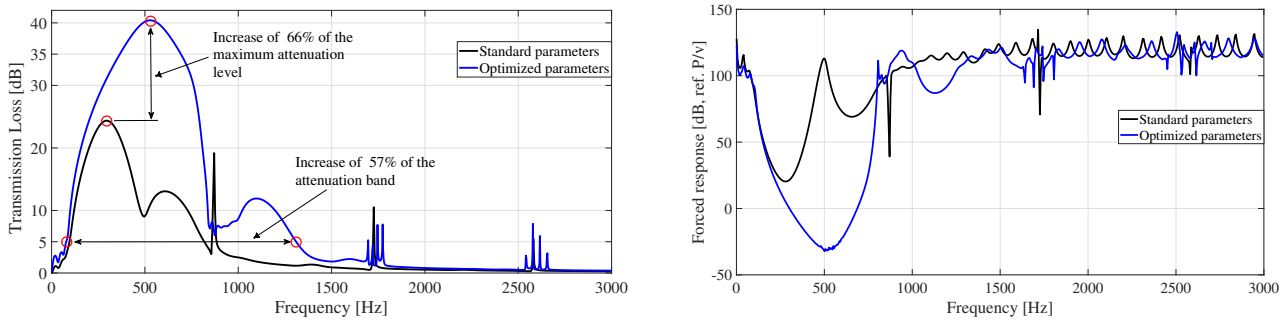

(a) Transmission loss (b) Forced response

Figure 8. Transmission loss curve for standard and optimized MPCM for the optimization of a graded-like finite structure.

5. CONCLUSIONS

The influence of the constructive parameters of micro-perforated chamber mufflers (MPCM) was investigated and the Differential Evolution (DE) method was implemented to optimize the design of MPCM silencer considering 4 different building/arrangements cases. The transmission loss and forced response curves were computed for all cases while the

dispersion diagram was computed for the infinity periodic case. All results have shown a considerable improvement in the acoustic performance of the MPCM silencer increasing the attenuation level. For the case 3 and 4, where a finite non-periodic structure was analyzed, it was also observed an increase on the attenuation bandwidth. In particular, the most noticeable improvement was observed for case 4 where the graded-like finite structure was optimized. Showing the potential of graded/rainbow metamaterial on the sound control. Also, the optimization process exhibited the potential of the DE algorithm on the design process for absorbing low-frequency noises, especially for frequency bands below 500Hz.

6. ACKNOWLEDGMENTS

The authors are grateful to the Brazilian research funding agencies CAPES Dinter UEMA-UNICAMP (Grant No. 23038.001802/2015-08), CNPq (Grant No. 313620/2018), FAPEMA (Grant No. BD-08741/17) and FAPESP (Grant No. 16794-2/2019; Grant No. 15894-0/2018) for the financial support.

7. REFERENCES

Allam, S. and Abom, M., 2011. "A new type of muffler based on micro-perforated tubes". *Journal of Vibration and Acoustics*, Vol. 133, No. 1.

Bilal, M.P., Zaheer, L.G.H.H. and Abraham, A., 2020. "Differential evolution: Areview of more than two decades of research". *Engineering Applications of Artificial Intelligence*, Vol. 90.

Bravo, T., Mauric, C. and Pinhède, C., 2016. "Optimisation of micro-perforated cylindrical silencers in linear and nonlinear regimes". *Journal of Sound and Vibration*, Vol. 363, No. 1, pp. 359–379.

Chen, W., Lu, C. and Liu, Z., 2020. "Optimal design of a 3d printed composite micro-perforated silencer for engine intake noise control". *IOP Conference: Materials Science and Engineering*, Vol. 774.

Fabro, A.T., Beli, D., Fergunson, N.S., Arruda, J.R.F. and Mace, B.R., 2021. "Wave and vibration analysis of elastic metamaterial and phononic crystal beams with slowly varying properties". *Wave Motion*, Vol. 103.

Goto, A.M. and Santos, J.M.C.D., 2019. "Sound attenuation of periodic micro-perforated chamber mufflers using transfer matrix method". In *Proceedings of XL CILAMCE*. Natal, RN-Brazil.

Hu, G., Austin, A.C.M., Sorokin, V. and Tang, L., 2021. "Metamaterial beam with graded local resonators for broadband vibration suppression". *Mechanical Systems and Signal Processing*, Vol. 146.

Kim, D.Y. and Ih, J.G., 2020. "Wideband reduction of in-duct noise using acoustic metamaterial with serially connected resonators made with mpp and cavities". *Applied Physics Letters*, Vol. 116.

Langley, R.S., 1995. "Wave transmission through one-dimensional near periodic structures: Optimum and random disorder". *Journal of Sound and Vibration*, Vol. 188, No. 5, pp. 717–743.

Lu, C., Chen, W., Liu, Z., Du, S. and Zhu, Y., 2017. "Pilot study on compact wideband micro-perforated muffler with a serial-parallel coupling mode". *Applied Acoustics*, Vol. 115, No. 1, pp. 15–22.

Maa, D.Y., 1975. "Theory and design of micro-perforated panel sound-absorbing constructions". *Scientia Sinica*, Vol. 18, No. 1, pp. 55–71.

Maa, D.Y., 1987. "Microperforated-panel wideband absorbers". *Noise Control Engineering Journal*, Vol. 29, pp. 77–84.

Maa, D.Y., 1998. "Potential of micro-perforated panel absorber". *The Journal of the Acoustical Society of America*, Vol. 104, No. 1.

Meng, H., Chronopoulos, D., Fabro, A.T., Elmadih, W. and Maskery, I., 2020. "Rainbow metamaterials for broadband multi-frequency vibration attenuation: Numerical analysis and experimental validation". *Journal of Sound and Vibration*, Vol. 465.

Shi, X. and Mak, C.M., 2017. "Sound attenuation of a periodic array of micro-perforated tube mufflers". *Applied Acoustics*, Vol. 115, No. 1, pp. 15–22.

Silva, P.B., Mencik, J.M. and Arruda, J.R.F., 2016. "On the use of the wave finite element method for passive vibration control of periodic structures". *Advances in Aircraft and Spacecraft Science*, Vol. 3, No. 3, pp. 299–315.

Storn, R. and Price, K., 1997. "Differential evolution - a simple and efficient heuristic for global optimization over continuous spaces". *Journal of Global Optimization*, Vol. 11, pp. 341–359.

Sullivan, J.W. and Crocker, M.J., 1978. "Analysis of concentric-tube resonators having unpartitioned cavities". *The Journal of the Acoustical Society of America*, Vol. 64.

Wu, M.Q., 1997. "Micro-perforated panels for duct silencing". *Noise Control Engineering Journal*, Vol. 45, No. 2.